Use of proton-transfer-reaction mass spectrometry to characterize volatile organic compound sources at the La Porte super site during the Texas Air Quality Study 2000

Thomas Karl,[1] Tom Jobson,[2,3] William C. Kuster,[2] Eric Williams,[2] Jochen Stutz,[4] Rick Shetter,[1] Samuel R. Hall,[1] Paul Goldan,[2] Fred Fehsenfeld,[2] and Werner Lindinger[5]

[1] Proton-transfer-reaction mass spectrometry (PTR-MS) was deployed for continuous real-time monitoring of volatile organic compounds (VOCs) at a site near the Houston Ship Channel during the Texas Air Quality Study 2000. Overall, 28 ions dominated the PTR-MS mass spectra and were assigned as anthropogenic aromatics (e.g., benzene, toluene, xylenes) and hydrocarbons (propene, isoprene), oxygenated compounds (e.g., formaldehyde, acetaldehyde, acetone, methanol, C_7 carbonyls), and three nitrogen-containing compounds (e.g., HCN, acetonitrile and acrylonitrile). Biogenic VOCs were minor components at this site. Propene was the most abundant lightweight hydrocarbon detected by this technique with concentrations up to 100+ nmol mol^{-1}, and was highly correlated with its oxidation products, formaldehyde (up to ~40 nmol mol^{-1}) and acetaldehyde (up to ~80 nmol/mol), with typical ratios close to 1 in propene-dominated plumes. In the case of aromatic species the high time resolution of the obtained data set helped in identifying different anthropogenic sources (e.g., industrial from urban emissions) and testing current emission inventories. A comparison with results from complimentary techniques (gas chromatography, differential optical absorption spectroscopy) was used to assess the selectivity of this on-line technique in a complex urban and industrial VOC matrix and give an interpretation of mass scans obtained by "soft" chemical ionization using proton-transfer via H_3O^+. The method was especially valuable in monitoring rapidly changing VOC plumes which passed over the site, and when coupled with meteorological data it was possible to identify likely sources.   INDEX TERMS: 0322 Atmospheric Composition and Structure: Constituent sources and sinks; 0345 Atmospheric Composition and Structure: Pollution—urban and regional (0305); 0365 Atmospheric Composition and Structure: Troposphere—composition and chemistry; KEYWORDS: PTR-MS, VOC, air quality, Houston, ozone

1. Introduction

[2] The greater Houston-Galveston metropolitan area is characterized by a high diversity of sources of volatile organic compounds (VOCs), carbon monoxide (CO) and nitrogen oxides (NO$_x$). This is especially true for the Ship Channel that connects the two cities, as it has a high density of petroleum refineries, synthetic organic chemical manufacturing plants and various mobile sources. As a consequence, a great portion of potential O_3 precursors released within and around the Ship Channel cause not only relatively high ozone formation rates but also highly variable ozone concentrations. The unique VOC mix in and around Houston represents a major difference to other metropolitan areas such as Nashville, Los Angeles and New York [Goldan et al., 2000; Kleinman et al., 2002], which have been the focus of previous field studies to assess urban air quality. The observed VOC/NO$_x$ ratios around Houston for example are significantly larger than expected from emission inventories and when compared to ratios obtained in other urban areas in the U.S. [Environmental Protection Agency (EPA), 1996]. Together with characteristic meteorological events such as the land-sea breeze flow reversal from the Gulf of Mexico, the complex chemical mixture in southern Texas leads to a persistent ozone problem, which typically led to 20 days of NAAQS (National Ambient Air Quality Standard) exceedances within a 3 month period

[1]Atmospheric Chemistry Division, National Center for Atmospheric Research, Boulder, Colorado, USA.

[2]Aeronomy Laboratory, National Oceanic and Atmospheric Administration, Boulder, Colorado, USA.

[3]Now at W. R. Wiley Environmental Molecular Sciences Laboratory, Pacific Northwest National Laboratory, Richland, Washington, USA.

[4]Department of Atmospheric Sciences, University of California Los Angeles, Los Angeles, California, USA.

[5]Insitut für Ionenphysik, Universität Innsbruck, Innsbruck, Austria.

during the COAST study in 1993 [*EPA*, 1996]. Ground-level ozone is considered as one target pollutant for control by the Clean Air Act in affected U.S. urban areas. As Houston, TX is now generally recognized having the second highest ambient ozone problem among U.S. cities [*EPA*, 1996], there is a current interest in developing strategies to bring this area into compliance with the NAAQS. State Implementation Plans required for noncompliant regions have to be based on a detailed knowledge of key-variables that govern ozone formation. VOCs in a high NO_x environment act as 'fuel' in the process of ozone production and thus are considered as target pollutants [*Chameides et al.*, 1992; *Sillman*, 1999].

[3] VOC monitoring at the La Porte site during the Texas Air Quality Study 2000 (TexAQS2000, available at www.utexas.edu/research/ceer/texaqs/) addressed several issues. These included: (a) assessment of the main VOC reactivity in and around the Ship Channel; (b) documentation of large, unscheduled VOC releases near the Ship Channel, that might contribute to unusually high-ozone events; (c) determination if the high observed VOC/NO_x ratios are due to inaccurate emission estimates of VOCs or NO_x; (d) evaluation of the importance of biogenic VOCs; (e) comparison of measured VOC concentrations with existing emission inventories; and (f) estimation of the magnitude of VOCs released by various point sources in the Ship Channel.

[4] Several techniques for measuring VOCs were utilized at the La Porte site. GC and GC-ITMS systems from the NOAA Aeronomy Laboratory, a GC-MS system from the University of Miami and a Proton-Transfer-Reaction Mass Spectrometry (PTR-MS) system from the University of Innsbruck were used to identify and quantify the VOC mixture during the whole intensive period between August 18 and September 17 2000. Here we will present results obtained by PTR-MS. This relatively new technique [*Lindinger et al.*, 1998] has been successfully employed for VOC analysis in various other field campaigns, such as LBA-CLAIRE [*Williams et al.*, 2001], INDOEX [*Warneke and de Gouw*, 2001] and SOS [*Stroud et al.*, 2002]. At La Porte the PTR-MS system allowed us to monitor VOCs in a continuous mode and detect trace constituents down to ~30 pptv. Principal component analysis (PCA) of the data set obtained during the TEXAQS 2000 field study helped to identify various sources for aromatic compounds in the Ship Channel and Harris County and distinguish between different anthropogenic emissions. In addition an assessment of the selectivity of this on-line technique and an interpretation of mass scans inferred from 'soft ionization' via H_3O^+ in a complex urban and industrial VOC matrix was undertaken.

2. Site Description and Experimental Details

[5] VOC analysis equipment (NOAA GC-ITMS, NOAA GC-FID, Miami GC-MS and PTR-MS) were placed in two air conditioned trailers situated next to a 10 m sampling tower at the south-west side of the municipal airport at La Porte, TX. The intercomparison between the different VOC sampling systems at the La Porte site allowed testing each individual technique for sampling losses and interferences (W. C. Kuster et al., An intercomparison of volatile organic carbon measurement techniques and data at the La Porte site

during TexAQS2000, submitted to *Environmental Science and Technology*, 2003, hereinafter referred to as Kuster et al., submitted manuscript, 2003). The sampling tower also housed several other analytical instruments for the determination of peroxynitrates (NOAA) [*Roberts et al.*, 2003], PAN, HNO_3, $RONO_2$ (UC Berkeley), HO_x (PSU) [*Martinez et al.*, 2002], phtotolysis frequencies (NCAR) [*Shetter and Mueller*, 1999], meteorological data, ozone, NO_x, SO_2, NO_y and CO (NOAA) and was managed by the NOAA Aeronomy Laboratory. Air was pulled through a 20 m glass manifold (i.d. 10 cm) down from the top of the sampling tower at a high pumping speed, reducing the pressure inside the manifold by ~60 mbar. All VOC experiments sampled from this manifold and were located 12–15 m downstream. A 10 m PFA-Teflon line (i.d. 1/4 inch) pumped by a diaphragm pump (Pfeiffer, MD4) at a pumping speed of ~30 l min^{-1} was used to bypass part of this air stream into the trailer. At its end a pressure controlled Teflon line (i.d. 0.0625 inch, length 1 m) led 15 sccm of this air stream into the PTR-MS instrument. The pressure in the 10 meter PFA-line was reduced to 500 mbar in order to avoid condensation inside the trailer, minimize memory effects and assure a fast response time. The overall response time caused a delay time of less than 5 s, measured by spiking a methanol pulse at the top of the tower. Leak tests at the glass manifold were performed using methanol and the fast monitoring capabilities of the PTR-MS instrument before continuous VOC monitoring at La Porte started.

[6] The PTR-MS instrument has been described in detail elsewhere [*Lindinger et al.*, 1998]. Briefly, the basic principle involves the mixing of a flowing air sample in a drift tube equipped with a source of H_3O^+ ions. H_3O^+ does not react with any of the main components of air (i.e., N_2, O_2, CO_2), as they all have lower proton affinities than H_2O, but H_3O^+ performs proton transfer to most VOCs in nondissociative reactions,

$$H_3O^+ + VOC \xrightarrow{k} VOCH^+ + H_2O \qquad (1)$$

[7] The proton transfer rate constants k are large, corresponding to the collisional limiting values ($\approx 10^{-9}$ cm^3 s^{-1}) [*Praxmarer et al.*, 1994]. The value for E/N (E being the electric field strength and N the buffer gas density) in the drift tube is kept at about 123 Townsend (Td) high enough to avoid strong clustering of H_3O^+ ions with water. The sensitivity of the PTR-MS instrument during the TEXAQS 2000 field study was typically on the order of 70 Hz/(nmol/mol) (counts per second per nmol/mol) for acetone and 50 Hz/(nmol/mol) for methanol at 2.5 mbar buffer gas pressure with a reaction time of 110 µs and 4 MHz H_3O^+ ions. The detection limit (DL) for compounds investigated in this work was inferred from a signal-to-noise ratio (S/N) of 2 according to DL = 2 × SD_{blank}/sensitivity, with SD_{blank} being the standard deviation of background count rates. For a 5s (2s) integration time this resulted in theoretical detection limits around ~20 pptv (~58 pptv). The uncertainty of the concentration measurements based on (1) is estimated to be on the order of ±30%. Owing to the low proton affinity of formaldehyde (PA = 170.4 kcal/mol) the backward reaction via H_2O can become significant and thus lower the sensitivity for this compound as indicated by *Hansel et al.* [1997]. Knowing the reaction rate constants

for the forward (Kf) and backward (Kb) reactions at ~123 Td, the sensitivity loss was calculated according to

$$H_3O^+ + CH_2O \overset{Kf}{\underset{Kb}{\leftrightarrow}} CH_2OH^+ + H_2O, \qquad (2)$$

using K_f (2×10^{-9} cm³/s) and K_b (2×10^{-11} cm³/s) @ 0.15 eV (KE_{cm}) values reported by *Hansel et al.* [1997].

[8] The predicted sensitivity ($21 \pm 2\%$ at 40000 ppmv H_2O partial pressure in the drift tube) was subsequently calculated based on the forward and backward reaction rate constant, the measured H_2O partial pressure entering the drift tube from the ion source, ambient humidity and temperatures measured at LaPorte. The $(H_2O) \bullet (H_3O)^+$ cluster (reflecting ambient humidity) can be used for internal calibration of formaldehyde. Owing to the lower sensitivity of formaldehyde and higher background on m/z 31^+ the detection limit was on the order of $1-2$ nmol/mol. Unfortunately, a reliable formaldehyde calibration source was not available at the site. The calibration obtained for formaldehyde was therefore based on the predicted sensitivity (21%) multiplied by the calibration measured for acetaldehyde. A check on data quality was also performed during the study using daytime events when propene was the only dominant hydrocarbon (with neither ethene nor other hydrocarbons present, that would have a significant acetaldehyde yield). Assuming that the production of acetaldehyde and formaldehyde is dominated by photochemical destruction of propene, these cases should show a product yield according to the propene oxidation mechanism (acetaldehyde: formaldehyde ratio close to 1:1) and confirmed the calculated sensitivity of ~21%. In addition, the corrected formaldehyde data were compared with those independently inferred from the long path DOAS measurements for concentrations above 3 nmol/mol [2 m level; *Wert et al.*, 2003], yielding a slope of 0.9 ± 0.3 (R = 0.82), which is encouraging taking the two different sampling strategies and uncertainties due to the formaldehyde correction into account. The same calibration factors were used for estimating hydrogen cyanide (HCN) concentrations, with a similar low proton affinity (170.4 kcal/mol) [*Holzinger et al.*, 1999]. For most other compounds the calibration was additionally based on VOC concentration standards provided by the NOAA Aeronomy Laboratory, with an estimated uncertainty of ±20%. Reference measurements were taken through a catalytic converter (platinum wool at 430°C) and were performed every 30 min to 2 h.

[9] VOC monitoring using the PTR-MS started on August 18 and continued until September 11 (2000). The PTR-MS was operated in a full mass scan mode (20–220 amu) from August 18 until August 22 with a cycling rate of ~6 min/scan. The selective ion mode scanning through the most important compounds and providing a high time resolution (~30 s) was deployed on August 23–25, 28–29 and September 4–5 (2000). For the rest of the time (August 30–September 3, September 6–11) the instrument scanned up to 165 amu (cycling every 4.5 min) and covered the mass range of all major VOCs seen by this technique at the La Porte site.

3. Results

3.1. Local Meteorological Details

[10] Surface winds at La Porte were characterized by north-westerly winds in the early morning (0:00–7:00)

shifting during the day through north and dominating from ~100–250 degrees in the afternoon. This persistent diurnal cycle dominated almost throughout the whole measurement period (Figure 1). Wind speeds at 10 m during the night generally varied between 2 and 5 m s^{-1}, with a slight decrease in the early morning. Along with the developing boundary layer surface wind speeds increased around 9:00 and typically reached a maximum (6–8 m s^{-1}) during the afternoon and early evening (15:00 to 19:00). For wind speeds up to 4 m s^{-1} no distinct direction persisted and winds shifted corresponding to the daily land-sea breeze effect. Higher wind speeds (>4 m s^{-1}) usually dominated from SE to SW (~100–200 degrees) and generally occurred in the afternoon. Days with low ozone concentrations (e.g., August 28; ~50 nmol/mol) were usually related to winds from the south at wind speeds up to 9 m/s. High ozone concentrations (August 30 and 31; ~200 nmol/mol) occurred during days with a surface high-pressure region over the central Houston area drifting slowly to the southwest and causing low-level winds from south-west to northwest at wind speeds around 1–3 m s^{-1}. A heat wave during summer 2000 caused high daytime temperatures (35–42°C) during the whole intensive campaign. Nighttime temperatures usually cooled down to 22–24°C. Scattered thunderstorms occasionally caused heavy rain showers with wind speeds up to 20 m s^{-1} from various directions.

3.2. Observed Volatile Organic Compounds at La Porte

[11] Overall 28 ions dominated the mass spectra obtained by PTR-MS in August and September 2000. Compounds listed in Table 1 explain about 80% of the total VOC loading within the observed mass range (m/z 18^+–m/z 220^+) measured by this technique at La Porte. It is noted, however, that proton affinities for most alkanes (<C$_7$), some alkenes (<C$_3$) and alkynes (<C$_3$) are lower than H_2O and not ionized during proton-transfer via H_3O^+ (NIST). For many ions (methanol, acetone, acetaldehyde, formaldehyde, HCN, acrylonitrile, benzene, toluene, styrene and C$_3$–C$_5$ benzenes) the selectivity of the PTR-MS instrument was good enough to identify a single compound plus its isomers attributing to the observed ion-density. PTR-MS specificity has recently been reviewed elsewhere [*de Gouw et al.*, 2003; *Williams et al.*, 2001]. As an example, Figures 2a and 2b show an acetone and benzene intercomparison plot with the NOAA GC-Iontrap for the whole measurement period. Acetone and propanal are isomers and cannot be distinguished by the PTR-MS technique. The intercomparison here showed that the signal on m/z 59^+ (mass/charge ratio of 59) was primarily related to acetone, confirming results from previous field studies [*Warneke and de Gouw*, 2001, *Pöschl et al.*, 2001] and a detailed GC-PTRMS evaluation [*de Gouw et al.*, 2003]. The GC-MS sampled every hour with a trapping time of 10 min, thus when comparing this data set with a 5 min intermittently sampled (2 s integration time per mass) data set collected by the PTR-MS instrument, a natural scatter between both techniques will occur due to the different sampling strategies. However, the correlation coefficients R for the examples shown in Figure 2 were high, around 0.9. Table 1 shows the obtained slopes between the PTR-MS and complementary GC-FID and GC-Iontrap systems (T. B. Jobson et al.,
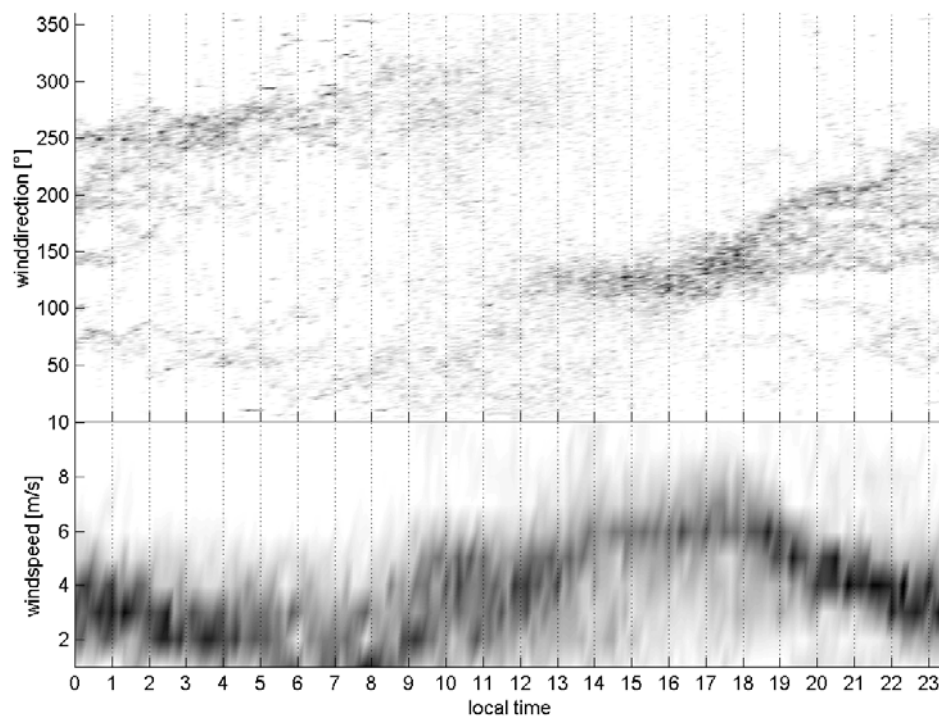
Figure 1. Diurnal plots of wind speed (lower panel) and wind direction (upper panel) during the whole study at La Porte, Texas. Darker shades represent more frequent occurrences.

Hydrocarbon source signatures in Houston, Texas: Influence of the petrochemical industry, to be submitted to *Geophysical Research Letters*, 2003). A more detailed discussion about mass spectral identification and intercomparison with complementary GC techniques is presented elsewhere (Kuster et al., submitted manuscript, 2003). Mean and maximum concentrations observed at La Porte are listed in the third column of Table 1. The high temporal variability of VOCs could easily result in a 2−4-fold concentration change in less than 10 min. As an example, Figure 3 depicts the variation of ambient concentrations for methanol (m/z 33^+), HCN (m/z 28^+), propene (m/z 43^+), MACR + MVK + C_5H_{10} (m/z 71^+), isoprene (m/z 69^+), $C_7H_{14}O$ (m/z 115^+), naphthalene (m/z 129^+) and C_6-benzenes (m/z 163^+) on August 23−24 2000. In general methanol (m/z 33^+) had the highest variations with ambient concentrations up to 574 nmol/mol. Individual propene plumes frequently resulted in mixing ratios around 100 nmol/mol. The proximity to local VOC sources was also demonstrated by anthropogenic isoprene (m/z 69^+). Two plumes coming in on August 23 at 10:45, just one hour after a heavy thunderstorm, increased isoprene levels up to 26.5 nmol/mol and 5 nmol/mol within a 90 min intervall. Although HO levels were around 7e6 molecules/cm^3 [*Martinez et al.*, 2002] methyl vinyl ketone (MVK) + methacrolein (MACR) (m/z 71^+) mixing ratios were comparably small in this case. Taking an upper limit for MVK + MACR concentrations of 1−4 nmol/mol (due to the possibility of direct emissions of MVK + MACR and potential interference of pentene isomers), wind speeds around 5 m/s and the measured OH-levels on that day ($\tau_{HO} \sim 17$ minutes) the isoprene source had to be within 0.5−4.4 km upwind. There are relatively little to no biogenic sources of isoprene in the proximity of the LaPorte site [*Wiedinmyer et al.*, 2001], leading to the conclusion that the measured isoprene came from a nearby anthropogenic source.

[12] In general the La Porte site was influenced by direct VOC emissions from nearby stacks, other fugitive industrial emissions and by automobile traffic. The VOCs of most interest to the TEXAQS 2000 study where light alkenes such as ethene, propene, C4 alkenes and aromatic compounds emitted form the petrochemical industry along the ship channel. Understanding the relative role of industrial and automotive alkene and aromatic compound emissions in driving ozone production during exceedances was a prime motivation for the study. A large fraction of the US ethene production capacity resides in Houston and large releases of ethene and propene into the atmosphere would have a significant impact on Houston's air mass reactivity. A thorough understanding of the industrial emissions inventory of these species (their magnitude, their temporal variability) will be essential for accurate photochemical modeling in Houston. While the PTR-MS is not sensitive to ethene, it was able to continuously monitor several masses associated with reactive alkenes: m/z 43^+, m/z 57^+, m/z 71^+, m/z 69^+. Figure 4a displays a time series of propene mixing ratios from the GC-FID and the PTR-MS signal at m/z 43^+. While the signal at m/z 43^+ can arise from the fragmentation of higher organics it is clear that elevated signals at this mass (up to 100 nmol/mol) where due to industrial propene emissions impacting the site. Major photoproducts from the OH-initiated oxidation of propene are formaldehyde and acetaldehyde in 1:1 yields. Formaldehyde (m/z 31^+) (CH_2O) and acetaldehyde (m/z 45^+) (CH_3CHO) were usually highly correlated in propene-enriched plumes also shown in Figure 4a. The PTR-MS
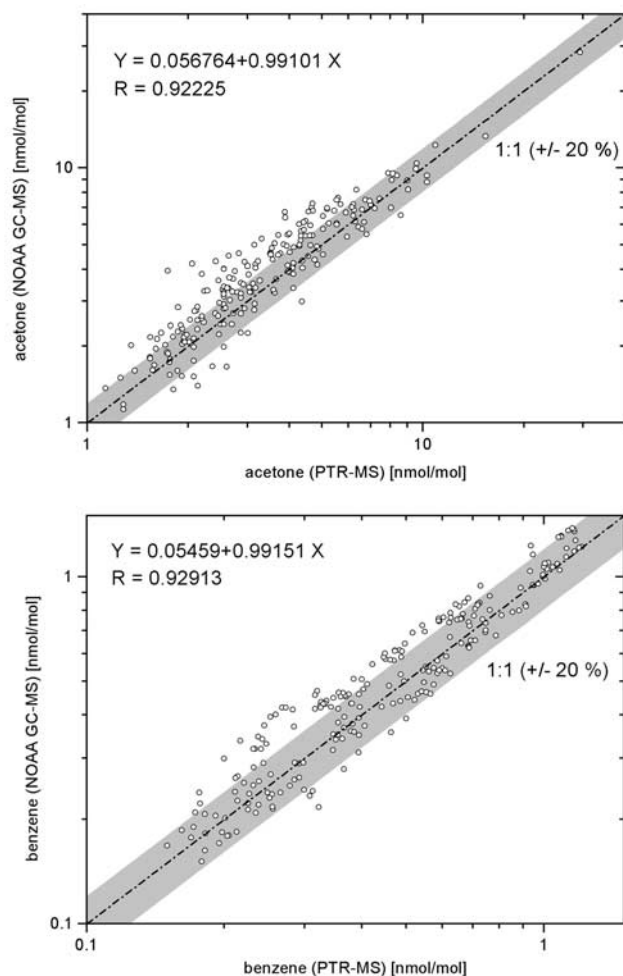
Figure 2. Intercomparison plot between the NOAA GC-Iontrap and the PTR-MS system for (a) benzene and (b) acetone for the entire measurement campaign.

formaldehyde data are in good agreement with formaldehyde measurements made by differential optical absorption spectrometry (DOAS) [*Geyer et al.*, 2003]. In this time series the regression of $\Delta CH_2O/\Delta CH_3CHO$ ratios is 0.84 ($R = 0.87$) approaching the 1:1 line expected as the yield from propene oxidation. The upper panel 1 of Figure 4a shows that at the beginning of the plume on August 25 high NO_x levels titrated ozone almost completely. The panel also depicts $j(O_3(1D))$ values, which reached ~40% of the daily maximum by 7:00 a.m. Increasing photolysis frequencies result in higher HO production rates and can account for an increased oxidation capacity. Figure 4b plots the ratio of CH_2O/C_3H_6 versus CH_3CHO/C_3H_6 for the plume on August 25 (black circles) and the whole data set (red open circles). A fairly compact trend is seen in both data sets. The propene plume data from August 25 defines a boundary in the data with the highest acetaldehyde/propene ratios, consistent with propene dominated chemistry. This is also illustrated by the reactivities shown in Figure 4a (middle panel). During the peak time of this plume (~8:30) propene accounts for as much as 70%, ethene 20% and higher alkenes (not shown) 10% of the total alkene reactivity. Propene photo-oxidation is likely to be a major source of

acetaldehyde in Houston, with ethene photo-oxidation being a major source of formaldehyde. Formaldehyde is also a product in the photoxidation of many VOCs, and it is not surprising that the bulk of the data display a higher HCHO/ propene ratio than the August 25 case.

[13] To assess the impact of ethene photochemistry on the trends observed, a simple box model analysis (using the NCAR Master Mechanism [*Hauglustaine et al.*, 1999; *Madronich and Calvert*, 1990]) was performed initialized with different starting ratios of ethene and propene and total starting concentrations of 100 nmol/mol. The model was run for several hours and used as a simple sequential reaction model with water vapor fixed at 7 g/kg and absolute NO_x fixed at 70 nmol/mol, but letting NO and NO_2 vary according to solar radiation. Background mixing ratios of the most important VOCs and CO were included, however no entrainment and dilution effects were assumed, since only the relative ratios between propene/formaldehyde and propene/acetaldehyde were investigated. Four cases (only C_3H_6 (gray line), $C_2H_4/C_3H_6 = 1:1$ (blue line), $C_2H_4/C_3H_6 = 3.4:1$ (purple line), inferred from measurements in the Lincoln tunnel [*Lonneman et al.*, 1986] and $C_2H_4/C_3H_6 = 5:1$ (green line)) reflect different emission scenarios. The regression for the plume on August 25 (black) falls close to the line inferred for propene dominated chemistry (gray) (Figure 4b). Together with the observed $\Delta CH_2O/\Delta CH_3CHO$ ratios and the calculated reactivities, it appears that the production of these light-weight aldehydes was dominated by propene initiated chemistry. Figure 4b
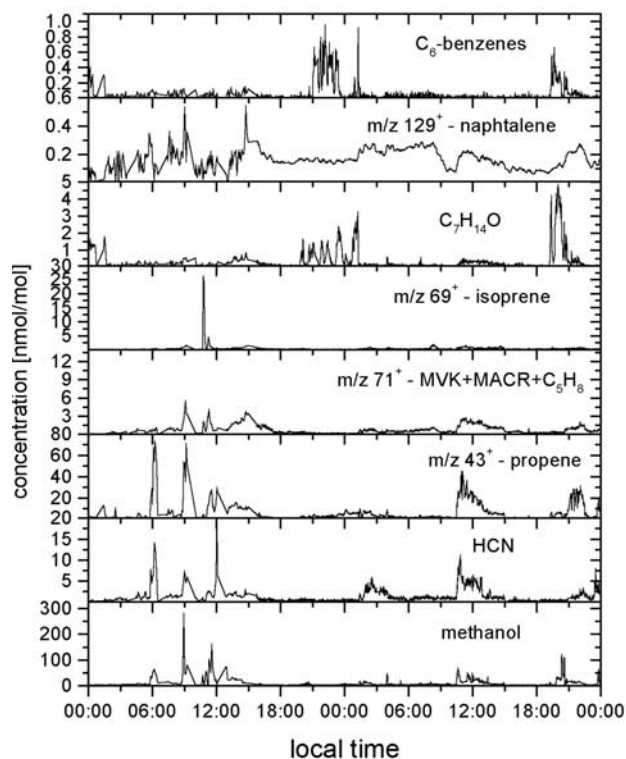

Figure 3. Ambient concentrations of methanol (m/z 33^+), HCN (m/z 28^+), propene (m/z 43^+), MACR + MVK + C_5H_{10} (m/z 71^+), isoprene (m/z 69^+), $C_7H_{14}O$ (m/z 115^+), naphthalene (m/z 129^+) and C_6-benzenes (m/z 163^+) on August 23–24 2000.

Table 1. List of Compounds Monitored by the Proton-Transfer-Reaction Mass Spectrometry Technique[a]

Compound	Monitored at Mass/Charge	Mean-Maximum Concentrations, nmol mol^{-1}	Slopes	Average OH Reactivity, s^{-1}	Source
Aromatic Compounds					
Benzene	M79	0.6–27.7	0.99[b]	0.02	I, U
Toluene	M93	0.8–13.0	0.98[b]	0.12	I, U
Styrene	M105	0.1–4.2	0.75[b]	0.14[c]	I
Xylenes	M107	0.6–6.4	1.10[b]	0.20[c]	I, U
C_3-Benzenes	M121	0.4–5.3	NA	0.22[c]	I, U
C_4-Benzenes	M135	0.2–6.6	NA	0.02[c]	I, U
Naphthalene	M129	0.13–0.8	NA	0.36	U, (I)
C_5-Benzenes	M149	0.02–0.5	NA	?	I,U
C_6-Benzenes	M163	0.03–1.0	NA	?	I, (U)
Hydrocarbons					
Propene	M43	6.3 (2.9)–212 (111)	b	2.14	I
Butenes + MTBE + butanol	M57	2.6 (0.64)–51.9 (42)	b	-	I
Pentenes + MVK + MACR	M71	0.8 (0.3)–7.2 (7.1)	b	-	I, O
Isoprene	M69	0.3 (0.3)–26.5 (28.8)	0.83[b]	0.57	I, (B)
C_6H_{10} + Hexanal	M83	0.2–6.1	NA	-	I
C_6H_{12}	M85	0.3–28.0	NA	-	I
C_7H_{12}	M97	0.2–3.8	NA	-	I
Oxygenated Compounds					
Methanol	M33	10.8–574	NA	0.24	I, (B)
Formaldehyde	M31	5.9–39.6	0.90	1.6	O
Acetaldehyde	M45	3.4–79	0.77	1.3	O, I
Acetone	M59	4.0–69	0.99[b]	0.02	I
$C_2H_4O_2$	M61/M43	3.4–67.9	NA	-	I, (O)
$C_4H_6O_2$	M87/M61/M43	0.5–9.2	NA	-	I
$C_4H_{10}O_2$	M91/M73	0.1–1.2	NA	-	I
$C_4H_8O_2$	M89	0.1–12	NA	-	I
$C_7H_{14}O$ (C_7-Ketones)	M115	0.4–155	NA	0.03[d]	I
N-Containing Compounds					
HCN	M28	1.4–27.0	NA	1e-4	I
Acetonitrile	M42	0.5–3.9	NA	2.7e-4	BB, I
Acrylonitrile	M54	0.4–56.8	NA	0.04	I

[a]Mean and maximum concentrations are given in the third column; in cases where isobaric interference for the hydrocarbon measurement could not be excluded, values (sum over all isomers) in parenthesis from the GC-FID measurements are given for comparison. The last two columns depict average reactivities using reaction rates from *Atkinson* [2000] and dominant source of pollution. I, industrial; U, urban/tailpipe/diesel; O, atmospheric oxidation product; B, biogenic; BB, biomass burning. Parentheses indicate minor source contribution.

[b]See complete intercomparsion between the 4 VOC techniques (Kuster et al., submitted manuscript, 2003).

[c]An average lumped reaction rate is used for these compounds.

[d]Value based on 3×10^{-12} cm^3 s^{-1}.

also plots the whole data set (red points) and assigns average times since the emission for the whole study assuming modeled HO concentrations (on average 4×10^6 molecules/cm^3) and photolysis rates (on average: 4×10^{-5} s^{-1} for CH$_2$O and 3×10^{-6} s^{-1} for CH$_3$CHO, comparable to measured maximum values on August 25 2000: 6.3×10^{-5} s^{-1} for CH$_2$O and 3.5×10^{-6} s^{-1} for CH$_3$CHO). Despite the fact that these times might not reflect cases in the early morning or late evening, it appears that the measurement site at LaPorte was close to the emission source in general. For the plume on August 25, measured HO concentrations for example increased from 1×10^6 molecules/cm^3 at ~7:50 LT to 4×10^6 molecules/cm^3 at 9:40 LT [*Martinez et al.*, 2002; G. J. Frost et al., Model-measurement comparisons of [OH], [HO2], and O3 production rate at La Porte Airport, Houston, during the 2000 Texas Air Quality Study, submitted to *Journal of Geophysical Research*, 2003, hereinafter referred to as Frost et al., submitted manuscript, 2003]. A more detailed study on the effects on model-measurement comparisons of HO, HO$_2$, and O$_3$ production rate can be found in the work of Frost et al. (submitted manuscript, 2003). In total

~64 hours (~156 hours), which accounts for ~11% (~27%) of the measurement period, were influenced by extremely (moderately) enhanced propene plumes with mixing ratios >10 nmol/mol (>5 nmol/mol) passing over the site. The overall correlation between CH$_2$O/C$_3$H$_6$ and CH$_3$CHO/C$_3$H$_6$, shows that more than 90% of the data fall within a 0:1 (propene case) and 5:1 C$_2$H$_4$/C$_3$H$_6$ (ethene/propene case) emission ratio, with photochemical ages between 15 min and 1.5 hours. Bias due to the presence of other reactive hydrocarbons leading to formaldehyde formation is comparably small as inferred from the GC-FID measurements. This supports the idea that (1) high propene/ethene emissions were close to the site, (2) their photochemistry plays a key role in the production of formaldehyde and acetaldehyde and (3) the total weighed OH reactivity from other hydrocarbons in propene/ethene plumes seemed to play a minor role.

[14] It is interesting to note some minor features observed on August 25: Even though not very reactive with respect to HO, methanol can cause some generation of formaldehyde at times when extremely high mixing ratios (up to several hundred nmol/mol) are present. Figure 4a (lower panel)
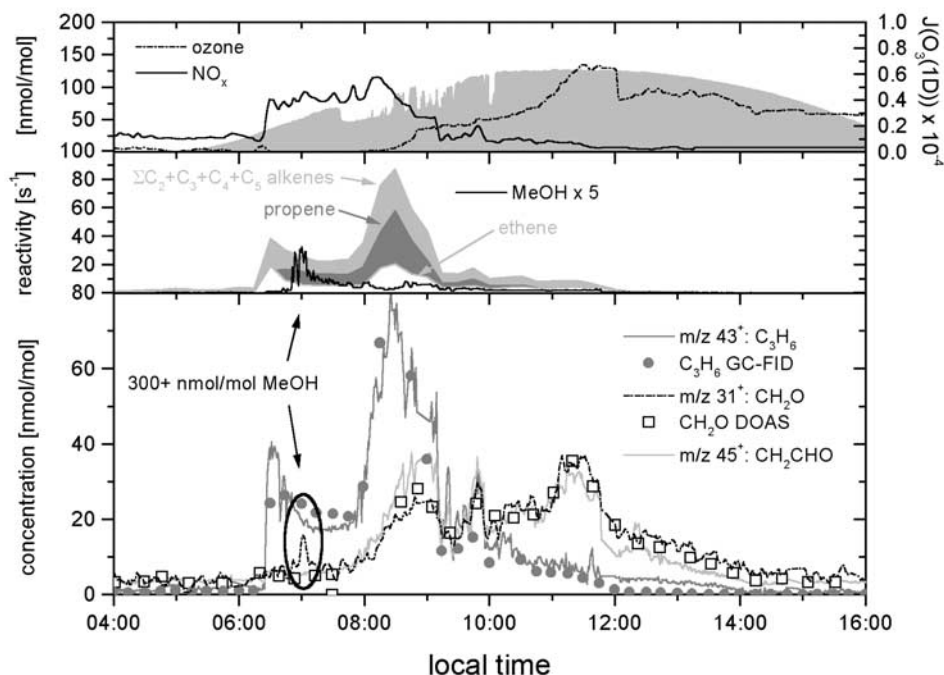
Figure 4a. Propene plume on August 25, 2000. Lower panel: propene (circles: GC-FID, solid line: PTR-MS), acetaldehyde (PTR-MS) and formaldehyde (PTR-MS, DOAS) concentrations measured by different techniques. Middle panel: reactivities of all alkenes (gray), propene (blue), ethene (dark blue) and methanol (cyan). Upper panel: $j(O_3(1D))$ (yellow shaded area), NO_x and ozone.
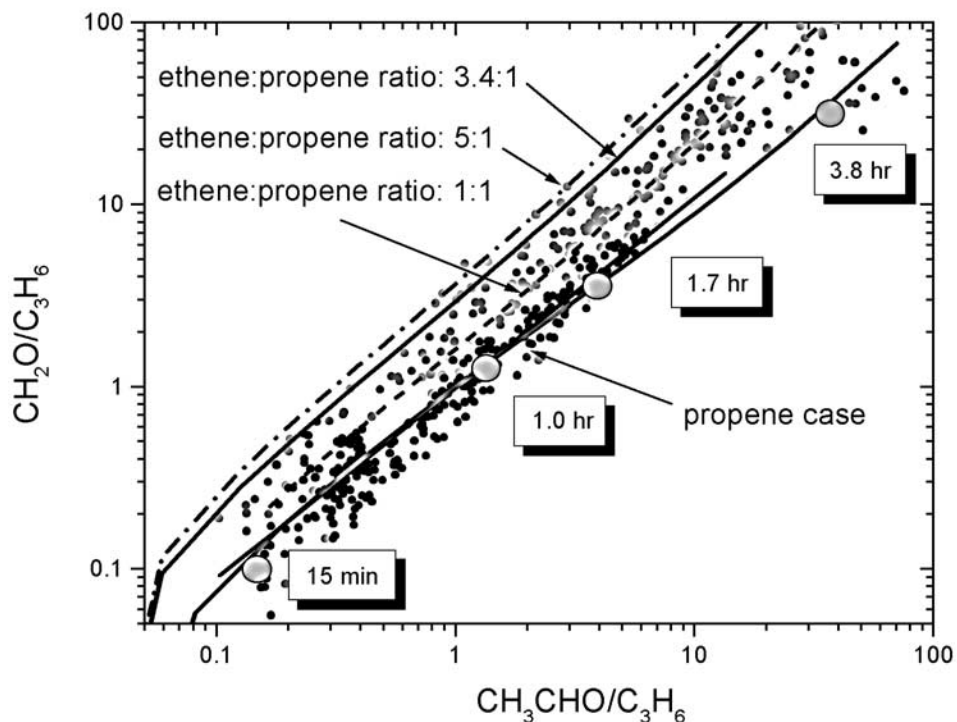

Figure 4b. The correlation of CH_2O/C_3H_6 plotted versus CH_3CHO/C_3H_6. (black circles: plume on August 25, red circles: whole study, gray line: expected ratio for a propene plume, blue line: ethene:propene = 1:1, purple line: ethene:propene = 3.4:1, green line: ethene:propene = 5:1). Average photochemical ages are derived assuming the output from the photochemical box model with average HO densities of 4×10^6 molecules/cm^3.

shows that formaldehyde concentrations increased from 5 to 15 nmol/mol around 07:00 LT. This coincided with a very large peak of methanol with concentrations of 300+ nmol/mol. The middle panel shows the reactivity of the major VOCs seen in this plume. Methanol (cyan) comprises almost 20% of the total reactivity of all alkenes (gray shaded area) dominated by propene and ethene. In order to assess the impact on formaldehyde concentration we assume HO concentrations between $1-4 \times 10^6$ molecules/cm^3 and photolysis rates of formaldehyde around 4×10^{-5} s^{-1}. Methanol at 300 nmol/mol could account for as much as $2-8$ nmol/mol formaldehyde two hours after emission. This can be compared to $1-4$ nmol/mol and $1-5$ nmol/mol, which would be generated by $20-30$ nmol/mol ethene and propene, respectively. The increased methanol concentrations can therefore account for part of the formaldehyde enhancement around 07:00 LT. The rest could be due to direct emissions of formaldehyde coinciding with methanol. Some datapoints in Figure 4b (between ratios of $0.1-1$) are therefore shifted toward higher formaldehyde/propene ratios. Column 5 in Table 1 lists average reactivities inferred from the VOC measurements during the whole study. It appears that the average reactivity of methanol (0.24 s^{-1}) is comparable to aromatic compounds ($0.1-0.22$ s^{-1}) and about half of isoprene (0.56 s^{-1}) suggesting that methanol at times can have some influence on the observed formaldehyde concentrations. One to two hours later ($08:00-09:00$ LT) acetaldehyde concentrations were slightly higher (36 nmol/mol) than those of formaldehyde (25 nmol/mol) (Figure 4a, lower panel). This enhancement can only partly be explained by C2-butene and T2-butene, which reached $\sim$2% of the propene abundancy and have large acetaldehyde yields (200%). Assuming average photochemical ages between 15 minutes and 1 hour (Figure 4b) and an average rate constant roughly 2.3 times that of propene, we estimate an upper limit of $2-4$ nmol/mol of acetaldehyde ($24-36\%$ of total acetaldehdyde enhancement) deriving from C$_4$ alkene oxidation. Because of the low abundancy of higher alkenes, the rest ($7-9$ nmol/mol) is most likely related to direct acetaldehyde emissions. The acetaldehyde enhancement causes a few datapoints in Figure 4b (between ratios of $0.1-1$), which are shifted to the right.

[15] To rationalize the observed measurements of propene, ethene, methanol, its reaction products and NO$_x$ in this plume, available emission inventories and upset reports were reviewed. The only upset on this day reported 5000 lbs of propene and 26 lbs NO$_x$, however 19050 lbs ethene. The GC-FID measurements on the other hand show that the ethene mixing ratios were as high as propene, implying that ambient mixing ratios observed in this particular case were due to 'business as usual' and to the fact that propene emissions were not reported quantitatively.

3.3. Statistical Data Analysis with Principal Component Analysis

[16] Benzene, toluene, C$_2$, C$_3$, C$_4$ - benzenes and styrene were among the most abundant aromatic species, monitored on m/z 79$^+$, 93$^+$, 107$^+$, 121$^+$, 135$^+$ and 105$^+$, respectively. As an example, Figure 5 demonstrates the variability of benzene, toluene and xylenes during the whole study. The high time resolution measurements of these species facilitated a statistical treatment using conventional principal component

analysis (see appendix) to identify common sources. From this analysis it was found that five factors explained 90% of the variability in these data. These five factors were labeled as: mobile source (MOB), benzene point source (H1), toluene point source (H2, ShC), mixed source (H3), and a styrene/xylene point source (xylene). Figure 6 shows the final source profiles for aromatic compounds and CO. The lower panel depicts relative ratios (the sum over all sources for one compound adds up to 100%), the middle panel absolute factor loadings (inferred from the covariance matrix) and the top panel the average OH reactivity (excluding the OH reactivity from CO). Large point sources of benzene, toluene and C$_2$-C$_4$-benzenes and styrene account for more than $\sim$60% of the total variance, based on the covariance. The mobile factor represents the typical signature of mobile sources with toluene/benzene ratios around 2 (as shown in the middle panel) consistent with reported values of approximately 1.8, [*Singer and Harley*, 2000] and explains around 37% of the variance. The high correlation with CO suggests that CO is mainly related to mobile sources at La Porte (benzene/CO = 9.8×10^{-4}). Comparison with data from Nashville [*Goldan et al.*, 2000] seems to support this idea, where the ratio between benzene and CO yielded approximately $(7 \pm 4) \times 10^{-4}$. A benzene source located in Harris, TX on Bay Area Blvd. was likely to be responsible for the benzene factor (H1), which has a high contribution when wind directions are from the south east (150 degrees), a toluene dominated source (H2, ShC) and a mixed source profile (H3) are related to the southerly sector as well, however also show a contribution from the Ship Channel. Styrene and C$_2$-benzenes combine in the last factor (Xylene), which had contributions from the Ship Channel and the area south of the airport. The similar patterns of this factor suggest origin from common industrial processes. The upper panel shows average reactivities (inferred from the source activity profiles; a lumped reaction rate for >C$_2$-benzenes was used) for these 5 different sources, ranging between 0.04 to 0.2 s^{-1} during August/September, 2000. The mobile factor accounts for $\sim$20% of the total OH reactivity (0.65 s^{-1}) for aromatic compounds (excluding CO). Taking the 25 most important VOCs and CO emitted from mobile sources [*Lonneman et al.*, 1986] the overall reactivity (0.53 s^{-1}) was subsequently scaled based on the mobile source profile (shown in Figure 6). The diurnal reactivity pattern of mobile sources is also based on this standardization.

3.4. Diel Profiles and Correlation with Meteorological Variables

[17] The high time resolution of VOC measurements allowed tracking individual plumes over La Porte and collecting a statistically representative data set that can be correlated with parameters such as the surface wind distribution. For many compounds simple wind directional plots already locate polluted sectors. In order to standardize the observations (24 days, $1-7$ minutes sampling interval) we applied the following general linear model (GLM):

$$\ln(c(i(t),j(t))) = a_1 + a_2 \cdot T(i(t),j(t)) + a_3 \cdot WD(i(t),j(t))$$
$$+ a_4 ws(i(t),j(t)) + wday_j + lt_i + wday_j : lt_i, \quad (3)$$

where, i stands for 1 hour values of the day (i = 1..24), j for the day of the week (j = 1: Mo-Fr, j = 2: Sa, Su and
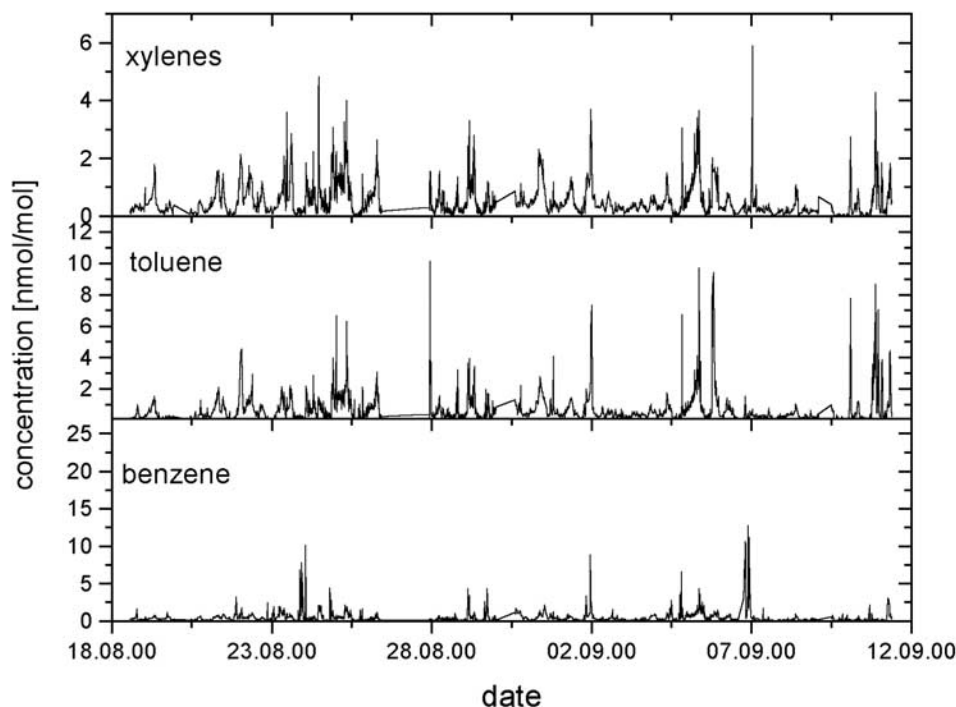
Figure 5. Benzene, toluene and xylenes mixing ratios for the whole measurement period.

holidays), t for time, T for temperature, WD for wind direction and ws for wind speed. The relative humidity was a perfect linear combination of ambient temperature and therefore not considered. Wday (j = 1: Mo-Fr, j = 2: Sa, Su and holidays), lt (local time: i = 1..24) and WD (0−360 are used as categorical variables for the day of the week and time of the day. The last term represents an interaction term, allowing different diurnal profiles. Since VOCs exhibited a lognormal distribution, the logarithm of ambient concentrations were used in the GLM. Diurnal profiles for various different sources, quantities and individual compounds are shown in Figures 7a, 7b, and 8.

[18] Figure 7a compares propene, the mobile source profile (SA: units are in nmol/mol for each aromatic compound after multiplied by the absolute factor loading obtained from Figure 6 middle panel), acrylonitrile and methanol plotted versus wind direction and local time and reflects the origin of different VOCs: propene (panel 1) usually dominates from NNE, whereas the mobile source profile (panel 2) (typically between 06:00−09:00 LT: see also Figure 7a, panel 3) is mainly related to emissions north of La Porte, where a major freeway (Pasadena Fwy 225) passes E-W. The fact that no evening rush hour peak was observed, was mainly due to afternoon winds from the SE-SW sector advecting relatively clean marine air from the Galveston Bay over La Porte (Figure 1). Acrylonitrile and methanol originate from the SC (NW) and a conglomerate of the synthetic organic industry located SE of the municipal airport. The right panels in Figure 7a depict mean reactivities of these compounds averaged over time and plotted versus wind directions, the upper panels show mean values averaged over wind directions and plotted versus time of the day. The reactivity of mobile sources was scaled according to VOC emission profiles reported by *Lonneman*

et al. [1986]. It is obvious that the OH reactivity is dominated by propene emissions with an average value up to $\sim$12.0 s^{-1} from the SC between 8:00−9:00 LT (mean over all wind directions is 2.3 s^{-1}, see also Table 1). The contribution of mobile sources adds up to $\sim$1 s^{-1}, aromatic compounds comprise about 22% of this amount. Peak values of methanol and acrylonitrile are as high as 0.3 s^{-1} (0.1 s^{-1}) and 0.1 s^{-1} (0.04 s^{-1}) respectively. The average reactivity in the afternoon (13:00−17:00) was dominated by propene (0.5−1 s^{-1}), other reactive hydrocarbons such as ethene and secondary photooxidation products (acetaldehyde and formaldehyde) (not shown). The mobile source, methanol and acrylonitrile accounted for 0.1−0.2 s^{-1}, 0.05−0.15 s^{-1} and 0.01−0.05 s^{-1}, respectively. Figure 7b shows a similar plot for the benzene (H1), toluene (H2,ShC) and mixed aromatic source (H3) profile and C$_7$H$_{14}$O. In order to calculate the concentration (nmol/mol) of each species lumped within the aromatic source profile, the source activity (SA) scale has to be multiplied by the absolute factor loading in Figure 6 (middle panel). It appears that the aromatic profiles shown in Figure 7b are emitted during nighttime from the south, where a conglomerate of the synthetic industry situated on Bay Area Blvd. could be identified as the most likely source. The toluene and mixed source profile also have a contribution from the ship channel, similar to propene. It is worth noting that the benzene source (H1) is located toward 150 degrees, whereas the toluene (H2, ShC) and mixed source profile (H3) show a southerly contribution from 180 degrees, in agreement with the major reported emission sources south of the Municipal Airport. The C$_7$H$_{14}$O carbonyl (uppermost panel, Figure 7b) seems to be primarily related to nighttime emissions. Wind-directionally averaged peak reactivities of the mixed, toluene and benzene source profiles are 0.2, 0.1 and 0.06 s^{-1}
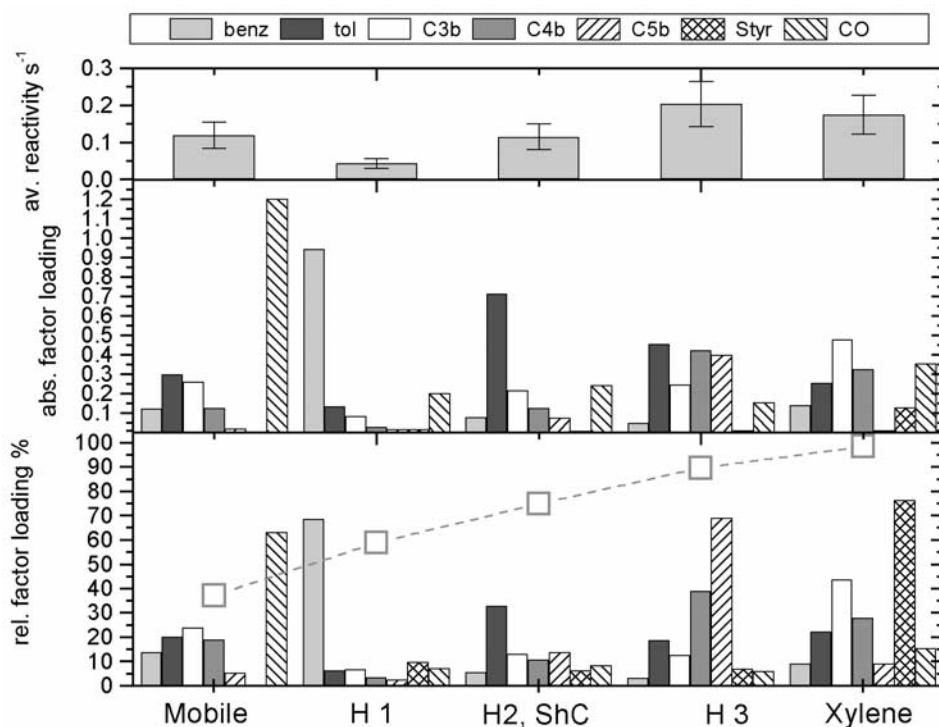
Figure 6. Results from PCA analysis for the most abundant aromatic species (benz: benzene, tol: toluene, C2b: Xylenes, C3b: C$_3$-benzenes, C4b: C$_4$-benzenes, Styr: styrene) together with carbon monoxide (CO). Lower panel: relative factor loadings (sum of each compound over all sources adds up to 100%) for different sources (mobile: tailpipe emissions, H1, H2, and H3: 3 different industrial sources south of the municipal airport in Harris County, ShC: industrial component from the ShipChannel, Styrene: Xylene and Styrene Factor); square symbols indicate the cumulative percentage of the total variance explained by the individual factors. Middle panel: absolute factor loadings (CO divided by 100). In order to calculate absolute concentrations (in nmol/mol) the absolute factor loading of each component (e.g., benzene) has to be multiplied by the source activity (SA) in Figures 7a, b and 8. Upper panel: average OH reactivity from each source (excluding the OH reactivity from CO).

respectively. The reactivity of C$_7$H$_{14}$O was based on a reaction rate constant of 3×10^{-12} cm^3/s and reached values up to 0.15 s^{-1}.

[19] Figure 8 shows diurnal plots of the mean boundary layer height (time averaged), the mobile source profile, ozone, formaldehyde, acetaldehyde and acetone, (averaged over wind directions using results obtained by equation 3). The mean boundary layer height, was ~300 m at 8:00 (local time) and thereafter steadily increasing until 15:00 (LT) with a maximum height of 1500 m. Ozone concentrations started to increase around 8:00 and reached a maximum in the afternoon between 14:00–18:00 (local time). Acetone, acetaldehyde and formaldehyde all increase about 1 hour after the rush hour peak (09:00–10:00 LT) mainly due to the fact that north to northeasterly winds dominated during these times mixing air from the Ship Channel south. Whereas acetone seems to stay at a constant level throughout the rest of the day, acetaldehyde and formaldehyde decrease in the afternoon, which could be due to their shorter lifetimes. The observations indicate that the latter two compounds are photochemically produced in substantial amounts in the ship channel due to alkene oxidation. Because of a limited data set of 4 weeks (3 weekends) some VOC profiles (such as the Ship Channel components) might not be represented adequately on weekends due to a mean

wind field dominating from southerly directions on these days.

3.5. Comparison with Toxic Release Emission Inventory

[20] The C$_7$-compound observed along with several aromatic species gives a typical signature from SE, where a conglomerate of the synthetic organic manufacturing industry is located within a distance of 2–5 miles. The region located SSW-SE of LaPorte was used as an example to assess the existing EPA emission inventory for aromatic compounds. Reported on-site emission rates (http://www.epa.gov/tri) of all aromatic compound processing plants located south of the municipal airport (Harris) were compared to observed VOC ratios in plumes from this area. A typical source profile of the SSW - SE sector was constructed based on information of the toxic release emission inventory (TRI) and upwind distance of all chemical plants listed for this sector. A Gaussian plume model [EPA, SCREEN 3] was used to calculate a worst-case scenario (stable nocturnal boundary layer and center of plume) for aromatic compounds, assuming that all plants were emitting this compound at the same time and that the relative contribution of each plant was only governed by the upwind distance. The EPA plume model would therefore predict a maximum
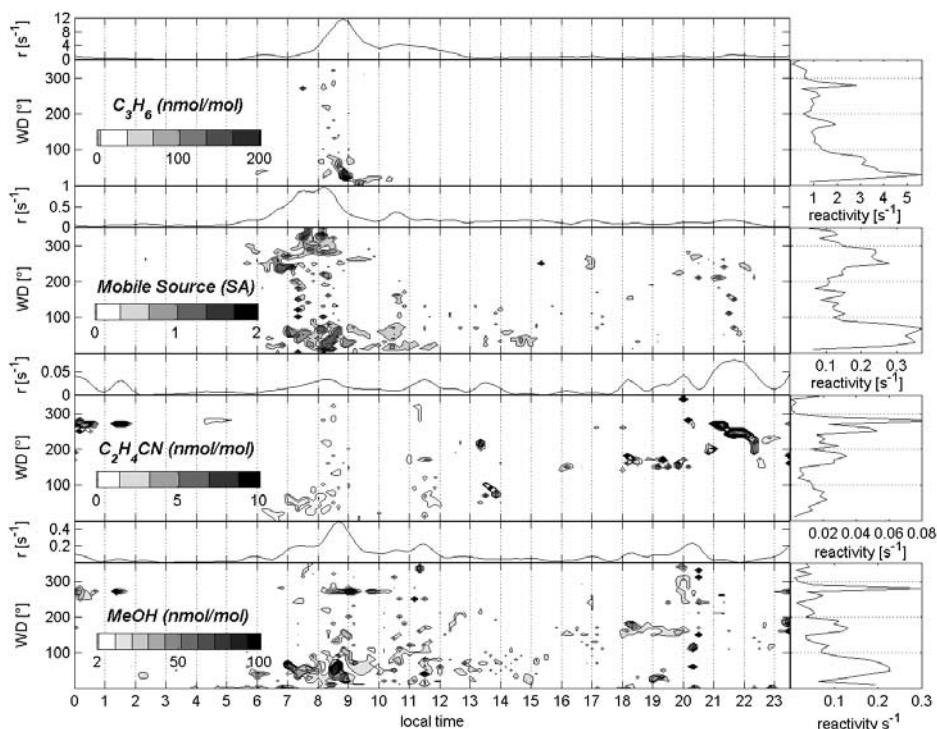
Figure 7a. Diurnal contour plot of methanol (MeOH), acrylonitrile (C_2H_4CN), the mobile source profile and propene (C_3H_6) plotted versus wind direction (y axis) and regressed according to equation (3). Right panels: time averaged reactivities of these 4 different sources plotted versus wind direction. Upper panels: wind directionally averaged reactivities of these 4 different sources plotted versus time of the day. The reactivity for the mobile source profile is scaled according to VOC emission ratios reported by *Lonneman et al.* [1986]. The units of the mobile source profile is given as a relative source activity (SA - nmol/mol), which when multiplied with the absolute factor loading of an individual component (e.g., benzene in Figure 6), reflects the concentration in nmol/mol of this compound.

concentration at the receptor given a specified emission rate (reported by the TRI emission inventory). The following parameters were used to initialize the model: source type (point), emission rate (g/s from TRI), stack height (10 m a.g.l.), stack inside diameter (2 m), stack gas exit velocity (0 m s^{-1}), stack gas exit temperature (310 K), ambient air temperature (293 K), receptor height (10 m a.g.l.), urban parameterization, no building downwash and full meteorology. The 'full meteorology option' is tuned toward the worst case. It provides therefore a sufficient but not necessary criterion for exceedances. If the measured concentrations always stayed below this predicted limit, the analysis would be inconclusive. However, at least for several cases the observed concentrations were much larger than the predicted worst-case scenario. Figure 9 summarizes the results together with those obtained by PCA analysis (Figure 6) using the sum over all measured mean source strengths from S - SE. Summing over all individual contributions resulted in predicted ambient mixing ratios (TRI) for example of ~4 nmol/mol for toluene (Figure 9 lower panel). On four occasions toluene concentrations from this sector were as high as 13 nmol/mol and on 16 occasions higher than 4 nmol/mol. The fact that no toluene upsets were reported during most of these periods (except on 08/27/00 and 08/28/00, when 1000 lbs of toluene emissions were reported, listed as upset #5697) suggests that reported yearly

emissions are either released intermittently (resulting in large VOC emissions at certain times) or that higher than reported amounts of this compound are regularly released into the atmosphere. Similar results were obtained for other aromatic compounds from this sector with peak values of 30, 22, 12, 9, 7 and 1 nmol/mol for benzene, toluene, C_2-benzenes, C_3-benzenes, C_4-benzenes and styrene, respectively. The relative ratios (upper panel) suggest that the emission inventory seems to over predict the toluene abundance compared to the rest. The square symbols indicate the relative uncertainty for the OH reactivity of aromatic compounds (released in the S - SE sector) due to the observed differences between measurement and emission inventory adding to a total of 45% (indicated by the dashed line). This means that if the total reported aromatic loading was correct, the emission inventory would still under predict the OH reactivity by 45%. This uncertainty partly arises from the fact that no C_4-benzenes are reported for this area. Strictly speaking the total uncertainty as used here has to be regarded as a relative measure and would add to a potentially larger bias if total emissions were under or overestimated.

4.   Conclusion

[21] Aromatic compounds were dominated by benzene, toluene and C_2–C_5 benzenes. About 20% of the aromatic
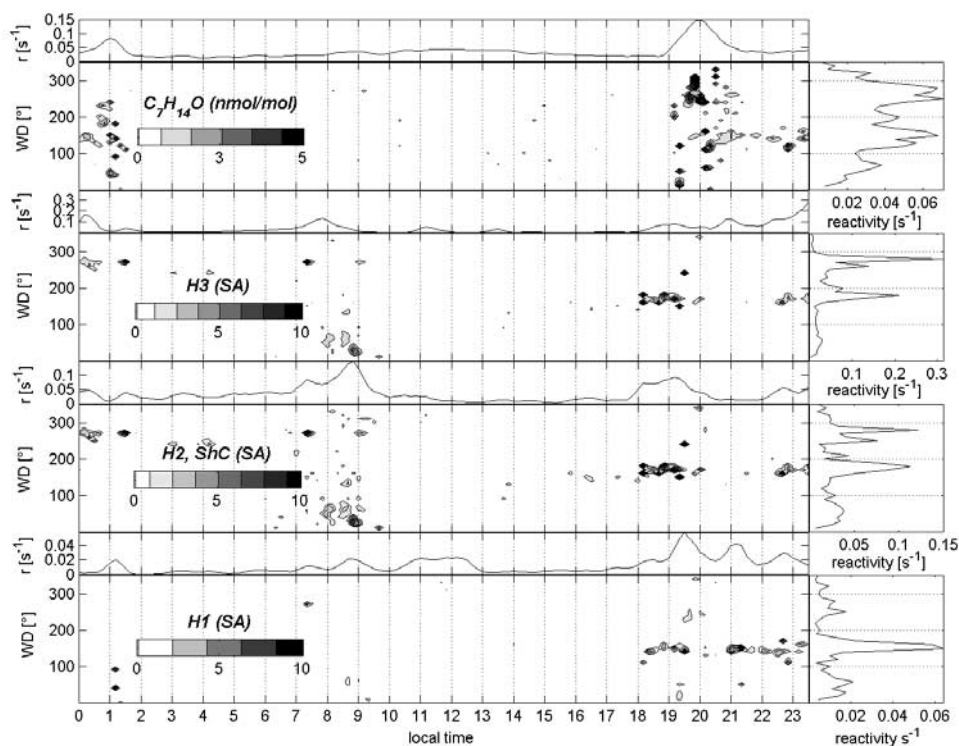
Figure 7b. Diurnal contour plot of source profiles H1, H2 +ShC, and H3 and $C_7H_{14}O$ plotted versus wind direction (*y* axis) and regressed according to equation (3). Right panels: time averaged reactivities of these 4 different sources plotted versus wind direction. Upper panels: wind directionally averaged reactivities of these 4 different sources plotted versus time of the day. The units of the aromatic source profiles are given as relative source activities (SA - nmol/mol), which when multiplied with the absolute factor loading of an individual component (e.g., benzene in Figure 6), represent the concentrations in nmol/mol of this compound.

OH reactivity and 37% of the observed variance was related to emissions from mobile (tailpipe) sources mostly released along the Pasadena Freeway passing E-W north of the Municipal airport. A conglomerate of the industries located south of the site caused strong point sources of aromatic compounds in the S-SE sector. Comparison with the Toxic Release emission inventory for the year 2000 suggests that the relative capacity of the OH reactivity for aromatic compounds from this sector is underestimated by 47%; this is mainly due to the fact that reported emissions for higher molecular weight benzenes (C_9 and C_{10}) are not correct and/or not included in the emission inventory. In addition frequent exceedances of benzene and toluene concentrations up to 10–27 and 4–13 nmol/mol suggest that absolute reported quantities seem to be underestimated and/or released intermittently resulting in large VOC releases at certain times. The fact that no upsets were reported in these cases suggests business as usual and if involving reactive species (e.g. xylenes or alkenes) could potentially contribute to ozone enhancements on a short timescale. Existing VOC databases completely lack emission factors for some higher molecular weight compounds, such as C_7- carbonyls, which were present up to 115 nmol/mol and primarily observed during nighttime. Therefore emission inventories currently used for regional air models in the greater Houston-Galveston area need to be carefully reevaluated and updated.

[22] The most abundant oxygenated compound was methanol with concentrations up to 574 nmol/mol. Though the reaction rate constant with OH is small, this compound together with potentially large emissions from live foliage [*Karl et al.*, 2002; *Karl and Guenther*, 2002] might add to an increased regional ozone precursor background. Peak concentrations of formaldehyde and acetaldehyde were both usually highly correlated with propene (the most abundant reactive hydrocarbon observed by the PTR-MS technique) and ethene and primarily related to emissions from refineries located northwest along the Ship Channel. The hydrocarbon measurements at La Porte suggest that tropospheric ozone production is most likely driven by low molecular weight alkene-NO_x chemistry, as shown for propene/ethene-dominated air masses advected south from the Ship Channel, supporting observations from aircraft measurements during TexAQS 2000 [*Ryerson et al.*, 2002; *Wert et al.*, 2003; *Kleinman et al.*, 2002]. Ozone control strategies will therefore also have to target VOC emissions. Acetone concentrations (4–69 nmol/mol) were usually enhanced in air masses originating from the Ship channel and related to primary industrial emissions and photochemical sources. Occasionally high concentrations of isoprene (up to ~27 nmol/mol) released by nearby anthropogenic sources were also seen at La Porte. Biogenic isoprene and mono-terpene concentrations at this site played a minor role. HCN
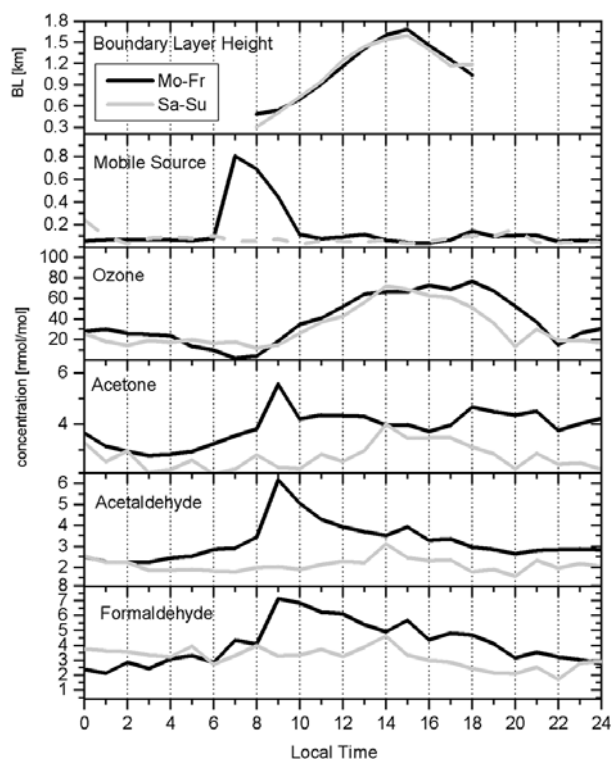
Figure 8. Diurnal profiles for the boundary layer height, mobile source profile, Ozone, acetone, acetaldehyde and formaldehyde. Concentrations are in nmol/mol except for the mobile source profile, which is plotted using a relative source activity (SA in nmol/mol) and has to be multiplied by the absolute factor loadings in Figure 6 in order to obtain the concentrations of individual compounds clustered within the profile.

and acrylonitrile were present in fairly high concentrations. These compounds might not be important players for local ozone chemistry, but can add to an increased regional VOC background and, considering their toxicity, may directly affect local air quality in and around the Shipchannel. Further data analysis using the recently developed multi-linear engine [*Paatero*, 1999; *Paatero and Hopke*, 2002] will help to extend the chemical mass balance modeling part and its implications to a broader range of compounds and industrial emissions (e.g., distinguish temperature driven, evaporative emissions from direct stack emissions). We conclude that the PTR-MS technique is a valuable tool for real-time VOC monitoring in a complex urban site, especially where there are rapidly changing plumes of VOCs released from industrial activities. Although PTR-MS technology does not allow detection of certain hydrocarbons (alkanes and ethene for example), its ability to monitor higher alkenes, aromatics, virtually all volatile oxygenates, and certain cyano-compounds, down to about 30 pptv attests to its versatility. Future PTR-MS deployments involving mobile systems could be used to track down local polluters, or simply help finding leaks in the vast pipeline network and storage facilities. It could therefore become an attractive technique for the chemical and refining industry as well as environmental protection agencies.

Appendix A

[23] Multivariate methods are widely used to estimate source-receptor relationships and are based on the mass conservation argument [*Henry et al.*, 1984; *Jackson*, 1991]. Chemical mass balance models (CMB) describe a linear relationship between source activities (S), the relative source strength of source p (a) and measured properties such as the ambient concentration (C)

$$C_{ik} = \sum_{j=1}^{p} a_{ij} \cdot S_{jk} + \varepsilon_k, k = 1 \dots m, \quad (A1)$$

where C_{ik} is the measured concentration of compound i at time k, a_{ij} the factor loading which is related to the source composition, S_{jk} the source activity and ε_k an error term to be minimized.

[24] There are many different methods for solving equation (A1) and extracting source profiles plus activities [*Henry et al.*, 1984]. Many CMB models often require information of the number of sources and their relative composition. Here we apply two complementary approaches for estimating source profiles, thus allowing cross-validation of the results. On the basis of equation (A1) the first method, similar to the
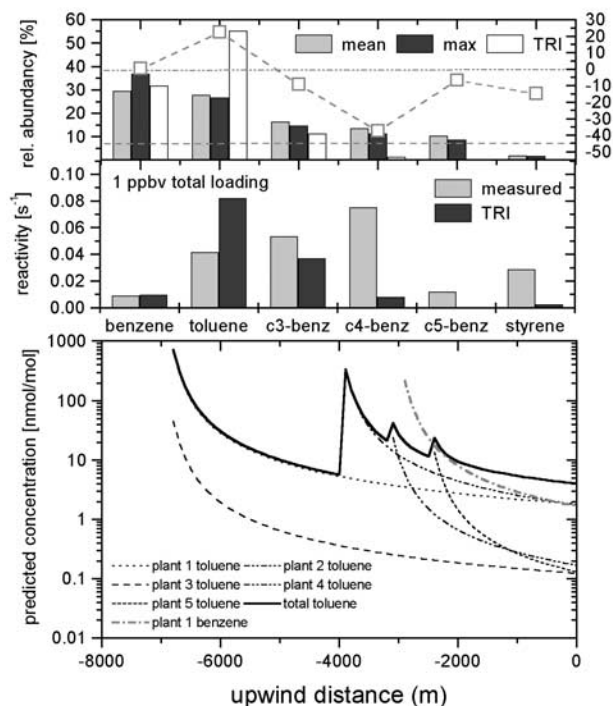

Figure 9. Assessment of the emission inventory for aromatic compounds. lower panel: results from a Gaussian plume model sensitivity analysis for toluene plants in the S-SE sector; middle panel: comparison between the measured and reported OH reactivity at 1 nmol/mol total aromatic loading; upper panel: relative abundancy of aromatic compounds emitted in the S-SE sector based on measured mean and maximum concentrations and reported emission rates listed in the toxic release inventory (TRI), square symbols (scale on the right side) indicate the relative uncertainty of the OH reactivity due to under and/or overestimation of individual compounds as listed by the TRI.

one proposed by *Staehelin et al.* [2001] applies a conventional principal component analysis (PCA) of the standardized data set. The first 5 principal components explained more than 90% of the variance and corresponded to the number of the most important sources; since every point of the transformed data set plotted in the new coordinate system can be assigned to the original observation, provisional source profiles can be obtained by locating different vortices bounding the data cloud. Corner points in the subspaces for example represent occasions where a single emission source was predominantly active. The second method for estimating provisional source profiles involved factor analysis (FA) of the covariance matrix using the 'VARIMAX' rotation originally introduced by Kaiser [*Jackson*, 1991].

[25] A common issue associated with multivariate techniques used in environmental problems is that appropriate transformations need to obey physical constraints, such as non-negative source compositions and activities. Here we use an alternating least squares regression minimizing negative contributions to obtain the final source profiles and activities. All calculations involving FA and PCA for extracting source profiles were done with Systat (SPSS 10) and MATLAB (version 5.3). It is noted that more sophisticated positive matrix factorization models, such as the multilinear engine [*Paatero et al.*, 1999], exist and will be used for further data analysis.

References

Atkinson, R., Atmospheric chemistry of VOCs and NO$_x$, *Atmos. Environ.*, *34*, 2063–2101, 2000.

Chameides, W. L., et al., Ozone precursor relationships in the ambient atmosphere, *J. Geophys. Res.*, *97*, 6037–6055, 1992.

de Gouw, J., C. Warneke, T. Karl, G. Eerdekens, C. van der Veen, and R. Fall, Sensitivity and specificity of atmospheric trace gas detection by proton-transfer-reaction mass spectrometry, *Int. J. Mass Spectrom.*, *223*, 365–382, 2003.

Environmental Protection Agency (EPA), National air quality and emissions trends report, 1995, *EPA 454/R-96005*, U. S. Government Print. Off., Washington, D. C., 1996.

Geyer, A., et al., Direct observations of First detection daytime of NO$_3$: Implications for urban boundary layer chemistry, *J. Geophys. Res.*, *108*(D12), 4368, doi:10.1029/2002JD002967, 2003.

Goldan, P. D., D. D. Parrish, W. C. Kuster, M. Trainer, S. A. McKeen, J. Holloway, B. T. Jobson, D. T. Sueper, and F. C. Fehsenfeld, Airborne measurements of isoprene, CO, anthropogenic hydrocarbons and their implications, *J. Geophys. Res.*, *105*, 9091–9105, 2000.

Hansel, A., W. Singer, A. Wisthaler, M. Schwarzmann, and W. Lindinger, Energy dependencies of the proton transfer reactions: H$_3$O$^+$ + CH$_2$O → CH$_2$OH$^+$ + H$_2$O, *Int. J. Mass Spectrom. Ion Processes*, *167*, 697–703, 1997.

Hauglustaine, D. A., S. Madronich, B. A. Ridley, S. J. Flocke, C. A. Cantrell, F. L. Eisele, R. E. Shetter, D. J. Tanner, P. Ginoux, and E. L. Atlas, Photochemistry and budget of ozone during the Mauna Loa Observatory Photochemistry Experiment (MLOPEX 2), *J. Geophys. Res.*, *104*, 30,275–30,307, 1999.

Henry, C. H., C. W. Lewis, P. K. Hopke, and H. J. Williamson, Review of receptor model fundamentals, *Atmos. Environ.*, *18*, 1507–1515, 1984.

Holzinger, R., C. Warneke, A. Hansel, A. Jordan, W. Lindinger, D. H. Scharffe, G. Schade, and P. J. Crutzen, Biomass burning as a source of formaldehyde, acetaldehyde, methanol, acetone, acetonitrile, and hydrogen cyanide, *Geophys. Res. Lett.*, *26*, 1161–1164, 1999.

Jackson, J. E., *A User's Guide to Principal Components*, John Wiley, Hoboken, N. J., 1991.

Karl, T., and A. Guenther, Eddy Covariance Measurements of Volatile organic compounds, Processes and mechanisms, paper presented at 7th Scientific Conference of the International Global Atmospheric Chemistry Project (IGAC), Int. Global Atmos. Chem. Proj., Crete, Greece, 2002.

Karl, T., C. Spirig, J. Rinne, C. Stroud, P. Prevost, J. Greenberg, R. Fall, and A. Guenther, Virtual disjunct eddy covariance measurements of organic compound fluxes from a subalpine forest using proton transfer reaction mass spectrometry, *Atmos. Chem. Phys.*, *2*, 999–1033, 2002.

Kleinman, L. I., P. H. Daum, D. Imre, Y.-N. Lee, L. J. Nunnemacker, S. R. Springston, J. Weinstein-Lloyd, and J. Rudolph, Ozone production rate and hydrocarbon reactivity in 5 urban areas: A cause of high ozone concentration in Houston, *Geophys. Res. Lett.*, *29*(10), 1467, doi:10.1029/2001GL014569, 2002.

Lindinger, W., A. Hansel, and A. Jordan, On-line monitoring of volatile organic compounds at pptv levels by means of proton-transfer-reaction mass spectrometry (PTRMS)-Medical applications, food control and environmental research, *Int. J. Mass Spectrom.*, *173*, 191–241, 1998.

Lonneman, W. A., R. L. Sella, and S. A. Meeks, Non-methane organic composition in the Lincoln Tunnel, *Environ. Sci. Technol.*, *20*, 790–796, 1986.

Madronich, S., and J. G. Calvert, Permutation reactions of organic peroxy radicals in the troposphere, *J. Geophys. Res.*, *95*, 5697–5715, 1990.

Martinez, M., et al., The behavior of the hydroxyl and hydroperoxyl radicals during TexAQS2000, *Eos Trans. AGU*, *83*(47), Abstract A12D-0174, 2002.

Paatero, P., The Multilinear engine-A table-driven, least squares program for solving multilinear problems, including the n-way parallel factor analysis model, *J. Comput. Graphical Stat.*, *8*(4), 854–888, 1999.

Paatero, P., and P. K. Hopke, Utilizing wind direction and wind speed as independent variables in multilinear receptor modeling studies, *Chemometrics Intelligent Lab. Syst.*, *60*(1–2), 25–41, 2002.

Pöschl, U., et al., High acetone concentrations throughout the 0–12 km altitude range over the tropical rainforest in Surinam, *J. Atmos. Chem.*, *38*, 115–132, 2001.

Praxmarer, C., A. Hansel, and W. Lindinger, Interaction between the ion dipole and the ion-induced dipole in reactions of the polar ion ArH$_3^+$, *J. Chem. Phys.*, *100*, 8884–8889, 1994.

Roberts, J. M., et al., An examination of the chemistry of peroxycarboxylic nitric anhydrides and related volatile organic compounds during Texas Air Quality Study 2000 using ground-based measurements, *J. Geophys. Res.*, doi:10.1029/2003JD003383, in press, 2003.

Ryerson, T. B., et al., Effect of petrochemical industrial emissions of reactive alkenes and NO$_x$ on tropospheric ozone formation in Houston, Texas, *J. Geophys. Res.*, *108*(D8), 4249, doi:10.1029/2002JD003070, 2002.

Shetter, R. E., and M. Mueller, Photolysis frequency measurements using actinic flux spectroradiometry during the PEM-Tropics mission: Instrumentation description and some results, *J. Geophys. Res.*, *104*, 5647–5661, 1999.

Sillman, S., The relation between ozone, NOx and hydrocarbons in urban and polluted rural environments, *Atmos. Environ.*, *33*, 1821–1845, 1999.

Singer, B. C., and R. A. Harley, A fuel-based inventory of motor vehicle exhaust emissions in the Los Angeles area during summer 1997, *Atmos. Environ.*, *34*, 1783–1795, 2000.

Staehelin, J., R. Locher, S. Moenkeberg, and W. A. Stahel, Contribution of road traffic emissions to ambient air concentrations of hydrocarbons: The interpretation of monitoring measurements in Switzerland by Principal Component Analysis and road tunnel measurements, *Int. J. Vehicle Design*, *27*(1–4), 161–172, 2001.

Stroud, C. A., et al., Nighttime isoprene trends at an urban forested site during the 1999 Southern Oxidant Study, *J. Geophys. Res.*, *107*(D16), 4291, doi:10.1029/2002JD000959, 2002.

Warneke, C., and J. A. de Gouw, Organic trace gas composition of the marine boundary layer over the northwest Indian Ocean in April 2000, *Atmos. Environ.*, *35*, 5923–5933, 2001.

Wert, B. P., et al., Signatures of alkene oxidation in airborne formaldehyde measurements during TexAQS 2000, *J. Geophys. Res.*, *108*(D3), 4104, doi:10.1029/2002JD002502, 2003.

Wiedinmyer, C., A. Guenther, M. Estes, I. W. Strange, G. Yardwood, and D. T. Allen, A land use database and examples of biogenic isoprene emission estimates for the state of Texas, USA, *Atmos. Environ.*, *35*, 6465–6477, 2001.

Williams, J., U. Poeschl, P. J. Crutzen, A. Hansel, R. Holzinger, C. Warneke, W. Lindinger, and J. Lelieveld, An atmospheric chemistry interpretation of mass scans obtained from a proton transfer mass spectrometer flown over the tropical rainforest of Surinam, *J. Atmos. Chem.*, *38*, 133–166, 2001.

_____

F. Fehsenfeld, P. Goldan, W. C. Kuster, and E. Williams, Aeronomy Laboratory, National Oceanic and Atmospheric Administration, Boulder, CO 80303, USA.

S. R. Hall, T. Karl, and R. Shetter, Atmospheric Chemistry Division, National Center for Atmospheric Research, Atmospheric Chemistry Division, Boulder, CO 80307, USA.

T. Jobson, William R. Wiley Environmental Molecular Sciences Laboratory, Pacific Northwest National Laboratory, Richland, WA 99352, USA. (Tom.Jobson@pnl.gov)

W. Lindinger, Insitut für Ionenphysik, Universität Innsbruck, A-6020 Innsbruck, Austria.

J. Stutz, Department of Atmospheric Sciences, University of California Los Angeles, Los Angeles, CA 90095, USA.